Nondissociative Electron Capture by Disulfide Bonds†

S. Carles, F. Lecomte, J. P. Schermann, and C. Desfrançois*

Laboratoire de Physique des Lasers, UMR 7538 CNRS - Université Paris-Nord, 93430 Villetaneuse, France

S. Xu, J. M. Nilles, and K. H. Bowen

Department of Chemistry, Johns Hopkins University, Baltimore, Maryland 21218

J. Bergès

Laboratoire de Chimie Théorique, UMR 7616 CNRS - Université Paris 6, 75005 Paris, France

C. Houée-Levin

Laboratoire de Chimie Physique, UMR 8600 CNRS - Université Paris-Sud, 91405 Orsay, France

Received: November 6, 2000; In Final Form: February 7, 2001

By means of Rydberg electron-transfer spectroscopy (RETS), negative ion photoelectron spectroscopy (NIPES), and quantum chemistry calculations, we have studied electron attachment properties of a series of saturated disulfides: dimethyl disulfide, diethyl disulfide, and dipropyl disulfide. Both RETS and NIPES experiments show that the valence anions of these disulfides are stable. RETS further shows that these negative ions result from attachment of nonzero energy electrons (0.2 eV), in contrast to dimers and larger complexes. NIPES experiments provide vertical detachment energies for the three disulfide monomer anions along with their Franck−Condon profiles. Fitting these spectra, using model potentials for the S−S stretch coordinate, finds that the adiabatic electron affinities of these disulfides are positive but rather small, about 0.1 eV. These experimental data compare well with the results of ab initio calculations, performed at the MP2 level with large basis sets.

1. Introduction

Covalent disulfide bonds are important determinants of the shapes of proteins, because S−S bonds between cysteines stabilize folded conformations.[1] In particular, it is now known that disulfide isomerases have chaperone activities,[2,3] disulfide bond formation being the activation transformation.[4] In addition, disulfide/dithiol redox systems control numerous important events in cellular life such as the regulation of cell growth and proliferation[5,6] and human cancer development.[7,8] More specifically, it has been shown that, in aqueous solution, protein disulfide radical anions are very stable,[9,10] and that the reduction of only one disulfide bridge does not necessarily modify the protein conformation.[11] Gas-phase studies of protein ions, using tandem mass spectrometry, have also provided useful information, including clues about the solution structures of disulfide-containing peptides,[12] the finding that some protein systems adopt different conformations in their disulfide-reduced vs their disulfide-oxidized forms,[13,14] and the recent demonstration[15] that low-energy capture by multiply charged protein ions induces selective dissociation at normally robust[16] disulfide bond sites. Reduction of disulfides is thus an important biological issue that deserves experimental and theoretical studies in order to be fully understood.

The problem we address here is that of low-energy electron capture, not by large peptide ions but by neutral model systems: a series of saturated disulfides R−S−S−R (R = CH_3, CH_3CH_2, $CH_3CH_2CH_2$). Formation of temporary dimethyl disulfide anions and stable fragmentation products, in free-electron collisions, has already been studied experimentally in dissociative electron attachment (DEA) experiments.[17] We here focus our attention upon nondissociative electron attachment by investigating the production and properties of intact and stable disulfide negative ions, by means of three complementary techniques: Rydberg electron-transfer spectroscopy (RETS), negative ion photoelectron spectroscopy (NIPES), and quantum chemistry (MP2 and DFT) calculations. RETS experiments determine whether our three model disulfides can attach low energy electrons and can lead to intact and stable anions in Rydberg electron-transfer collisions. NIPES experiments measure the electron binding energies of these anions, providing vertical detachment energies (VDEs). These experimental data are compared with quantum chemistry calculations that provide the molecular parameters of interest and help to interpret the experimental results. The formation of these disulfide anions is related to the general problem of three-electron bonds where a bonding σ molecular orbital is doubly occupied and its corresponding antibonding σ^* orbital is singly occupied. This situation has been considered previously in cyclic disulfide cation radicals[18] and in diatomic halogen anions.[19]

2. Experimental and Computational Techniques and Results

RETS experiments, performed at Paris-Nord University, are conducted by crossing a beam of laser-excited xenon atoms, in

† Part of the special issue "Edward W. Schlag Festschrift".

* Corresponding author: e-mail desfranc@galilee.univ-paris13.fr fax (33) 1 4940 3200.

10.1021/jp0040603 CCC: $20.00
Published on Web 03/22/2001

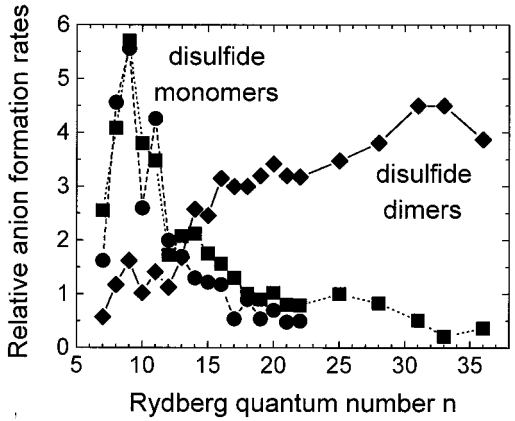

Figure 1. RETS data for the *n*-dependencies of the formation rates of monomer disulfide anions, dimethyl disulfide (squares) and dipropyl disulfide (circles), and dipropyl disulfide dimers (diamonds). Other monomers and dimers behave very similarly.

selected Rydberg states nf, with a supersonic beam of cold neutral disulfide molecules and clusters.[20] The sample beam is produced by flowing 2 bar of helium or argon over a room-temperature reservoir containing the studied disulfide, and the mixture is expanded through a pulsed 0.15 mm nozzle. The beam of xenon Rydberg atoms constitutes a source of electrons with well-controlled energy distributions in the 11 meV (n = 35) to 270 meV (n = 7) range. Anions, produced in charge-exchange collisions at the intersection of the two beams, under single-collision conditions are mass-analyzed in a linear time-of-flight setup, and their rates of creation are recorded as a function of the principal quantum number n of the selected Rydberg state. Fragment anions (RS^-, RSS^-, S^- and S_2^-), homogeneous cluster anions ($(RSSR)_N^-$), and mixed fragment-disulfide cluster anions are observed in the mass spectra. Only when helium is used as the carrier gas are intact monomer anions $RSSR^-$ also readily observed. This proves that these anions are stable against autodetachment, i.e., that the adiabatic electron affinity EA_{ad} of these disulfides must be positive. RETS data for the *n*-dependencies of the formation rates of disulfide monomer and dimer anions are presented in Figure 1. The main features of these data, which are interpreted in the next section, are the following. Monomer curves display a broad peak around n = 9 over a relatively low background which seems to go down almost to zero for high *n*-values, and monomer signals disappear when argon is used as the carrier gas. On the other hand, dimer curves possess a monotonic behavior, with almost constant formation rates for high Rydberg states, independently from the carrier gas.

While RETS is essentially an electron attachment technique, NIPES is an electron detachment method. NIPES experiments, performed at Johns Hopkins University, are conducted by crossing a mass-selected beam of cold negative ions with a fixed-frequency photon beam and by energy-analyzing the resultant photodetached electrons.[21] This is a direct technique for measuring anion electron binding energies and for obtaining other spectroscopic information about both neutral species and their corresponding anions. It is governed by the energy-conservation relationship, $h\nu$ = EBE + EKE, where $h\nu$ is the photon energy, EBE is the electron binding energy in the anion, and EKE is the kinetic energy of the photodetached electron. Because one knows $h\nu$ and measures the EKE spectrum, EBE is obtained by difference for each feature of the photoelectron spectrum. The anion source is a supersonic ion source in which electrons are injected from a floated filament directly into the

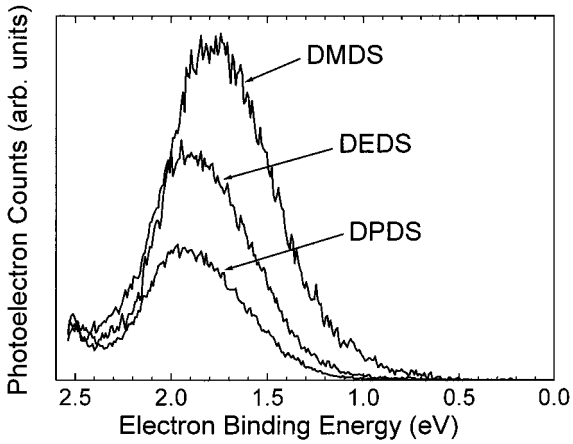

Figure 2. Negative ion photoelectron spectra of dimethyl disulfide (DMDS), diethyl disulfide (DEDS) and dipropyl disulfide (DPDS) anions. Vertical detachment energies (VDEs) are determined as the electron binding energies at the peak maxima (see Table 1).

TABLE 1: Vertical Detachment Energy (VDE), Vertical (EA_v), and Adiabatic (EA_{ad}) Electron Affinity Values of Several Disulfides, as Measured by NIPES and as Resulting from Ab Initio Calculations

disulfide molecule	VDE exptl (eV) NIPES	VDE theor (eV) MP2[a]/MP2[b]	EA_v theor (eV) MP2[a]	EA_{ad} theor (eV) DFT[a]/MP2[a]/MP2[b]
DMDS	1.75	1.58/1.69	−1.49	+0.35/−0.085/+0.12
DEDS	1.90	1.68/1.70	−1.45	+0.62/+0.058/+0.10
DPDS	1.92			

[a] 6-31+G* basis set. [b] 6-311+G(2d, 2p) basis set.

expanding jet in the presence of an axial magnetic field. For each of the three disulfides studied here, a few milliliters of a given disulfide was added to the stagnation chamber before it was closed and pressurized with argon gas to about 2 bar. The nozzle diameter was 17 μm. As in the RETS measurements, the disulfides were not heated, blending only their room temperature vapor pressure with the carrier gas in order to make a dilute mixture of disulfide in argon. The filament emission current was in all three cases very low, and the resultant parent ion signals quite high, thus strongly suggesting that these disulfide molecules possess positive adiabatic electron affinities. In addition, however, dissociative attachment products were also observed. The negative ions were mass-selected with a magnetic sector employing quadrupole doublets at both the entrance and exit slits of its flight tube. Once mass-selected, the anions were photodetached with about 100 circulating Watts of 488 nm (2.54 eV) photons from an argon ion laser operating intracavity. The photodetached electrons were then energy-analyzed with a hemispherical energy analyzer, having a resolution of about 30 meV. NIPES data for the anions of dimethyl disulfide (DMDS), diethyl disulfide (DEDS), and dipropyl disulfide (DPDS) are shown in Figure 2. Each of the three photoelectron spectra displays a broad Franck−Condon band around 1.2−2.2 eV, which will be interpreted in section 3. Qualitatively, this feature indicates that the geometric structure of the anions is different from that of their corresponding neutral. For each of these three anions, Table 1 tabulates the vertical detachment energy (VDE) values, taken as the EBE of the peak maximum. These values increase slightly as a function of the increasing length of the alkyl radical R.

Ab initio quantum chemistry calculations were performed at the IDRIS computing center of Paris-Sud University, using the Gaussian98 molecular orbital packages.[22] All neutral and anionic isolated species were optimized using large basis sets, 6-31+G*

TABLE 2: S-S Bond Dissociation Energies, D_e, Equilibrium Length, r_e, and Harmonic Frequency, $h\nu_e$

disulfide species	D_e (eV) MP2[a]/MP2[b]	r_e (Å) MP2[a]/MP2[b]	$h\nu_e$ (cm^{-1}) MP2[a]
DMDS neutral	2.45/2.68	2.056/2.071	526
	2.82[c]	2.038[d]	511[e]
DMDS anion	1.02/1.16	2.788/2.736	216
DEDS neutral	2.63/—	2.059/—	
DEDS anion	1.07/—	2.798/—	

[a] 6-31+G* basis set. [b] 6-311+G(2d, 2p) basis set. [c] Experimental value for D_0.[28] [d] Experimental value from microwave spectroscopy.[29] [e] Experimental value cited in ref 30.

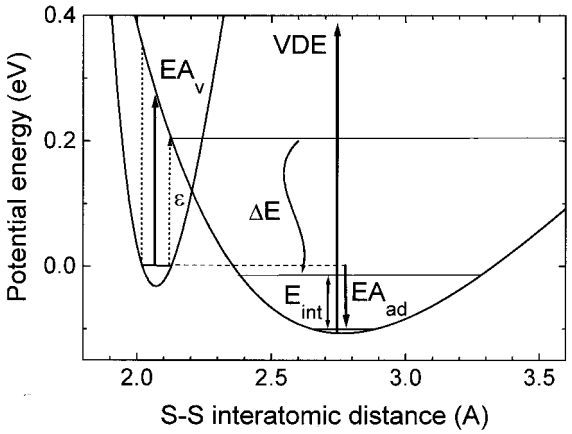

Figure 3. Sketch of the potential energy curves for the disulfide neutral and anion, as a function of the S−S bond length. In RETS experiments, electron attachment occurs, for a Rydberg electron energy ϵ, and nascent excited anions are further stabilized by the Rydberg core during the collision by an energy amount of ΔE slightly higher than ϵ. Observed stable anions are those that are left with an internal energy E_{int} slightly lower than the adiabatic electron affinity EA_{ad}. See text for discussion.

and 6-311+G(2d, 2p), at the second-order Moller−Plesset (MP2) perturbation level, because our previous studies[23] demonstrated the necessity of using such large basis sets. For comparison, density functional theory (DFT) calculations were also performed, using the B3LYP functional and the 6-31+G* basis set. Only DMDS and DEDS species were studied because these results suggest that very similar data would be obtained for DPDS. Results from these calculations are tabulated in Table 1 for VDE and EA values and in Table 2 for bond energies and interatomic S−S distances. Again, these results will be compared with experimental data in the next section, but we can immediately outline that the calculated VDEs are in good agreement with the NIPES data and that the EA_{ad} values, calculated with the larger basis set, are small but positive, also in agreement with the observation of stable monomer anions in both experiments.

3. Discussion

The shapes of the broad peaked RETS curves obtained for monomers are interpreted as follows. As suggested by theoretical results (see Table 1), the vertical electron affinities EA_v of disulfide molecules are probably negative so that the potential energy curve of the anion does not cross that of the neutral (+ electron at infinity) at zero energy, as depicted in Figure 3. Thus electron attachment cannot take place at nearly zero energy, and the creation rates fall off at very high n values, corresponding to Rydberg electrons of very low energy ϵ. When n decreases ϵ increases and electron-transfer begins to take place when the energy distribution of the outer electron in the Rydberg atom reach the Franck−Condon region, i.e., when ϵ approaches $-EA_v$. For very low n values, the formation rates may decrease again due to the lower geometrical cross-section of the Rydberg atom, which scales as n.[4] The observed peaked curve, for the monomer anion formation, can be thus interpreted as the result of these two competing processes. At the maximum, for $n = 9$, the mean Rydberg electron energy $\epsilon = 13.6\ eV/n^2$ is about 0.2 eV and electron attachment indeed occurs but probably on the low-energy edge of the Franck−Condon region, as discussed below. A value of −1.04 eV for EA_v has indeed been previously reported from DEA experiments,[17] and the present calculated value of −1.49 eV is even less negative. In the DEA data, fragment anion following electron attachment were, however, observed down to threshold electron energies as low as about 0.3 eV. On the other hand, the present n-dependencies for dimer and larger cluster anions display a monotonic behavior that is characteristic of s-wave attachment of very low energy electrons to a molecule in which EA_v is positive or zero.[24,25] This means that the solvation stabilization effect of a disulfide anion even by only one disulfide neutral is large enough so that the vertical electron affinity of the dimer becomes close to zero or positive. Because the solvation energy due to one polar molecule can hardly be greater than 0.5 eV, this is an indication that EA_v for monomer disulfides should be less negative than −0.5 eV.

Another important feature of the RETS experiments is that no monomer anion is observed when argon is used as the carrier gas, whereas other experimental conditions are identical and other cluster or fragment anions are still observed. This finding most probably results from the difference in collision energy, as interpreted here. Immediately after the electron transfer, Xe^+-DS^- complexes interacting via Coulombic forces are formed. The initial anion rovibrational internal energy is equal to the sum of the attached electron energy ϵ and the adiabatic electron affinity EA_{ad} (see Figure 3). During the remaining collision time, these unstable excited anions can convert a fraction ΔE of their internal energy into the translational motion of the Xe^+-DS^- system. When the Rydberg atom n-value decreases, ΔE increases and the nascent anions are more and more stabilized, because of the stronger interactions between Xe^+ and DS^-.[24,25] Anions eventually become energetically stable against autodetachment when their final internal energy E_{int} is lower than EA_{ad}, i.e., when ΔE becomes larger than ϵ. For n-values around 9, ϵ values are about 0.2 eV and energy transfers ΔE can hardly overcome this value.[24,25] It is thus likely that the observed anions are those that have resulted from electron attachment on the low-energy edge of the Franck−Condon region and which have been stabilized just enough below the autodetachment limit, i.e., with E_{int} just lower than EA_{ad}. This also could explain the relative weakness of monomer signals as compared to cluster signals. Moreover, depending on the initial relative collision energy E_k, the initial Rydberg atom ionization potential, IP_n plus E_{int}, and EA_{ad}, the Xe^+-DS^- ion pairs can then dissociate or not.[24,25] Namely, from energy conservation during the collision, ion pair dissociation will occur only if $E_k - IP_n$ is larger than $E_{int} - EA_{ad}$. Thus, observed anions also correspond to the fulfillment of the condition $E_k > IP_n - EA_{ad} + E_{int}$. When disulfide monomers are seeded in argon, the collision energy is about 0.08 eV, whereas it is above 0.5 eV in helium. Because IP_n is about 0.2 eV for n about 9, and because $E_{int} - EA_{ad}$ is only slightly negative, the above dissociation condition is always fulfilled in helium but it is not in argon.

We now come to the interpretation of NIPES experiments that were originally conducted in order to determine the adiabatic electron affinities of these disulfides. Prior to the present studies,

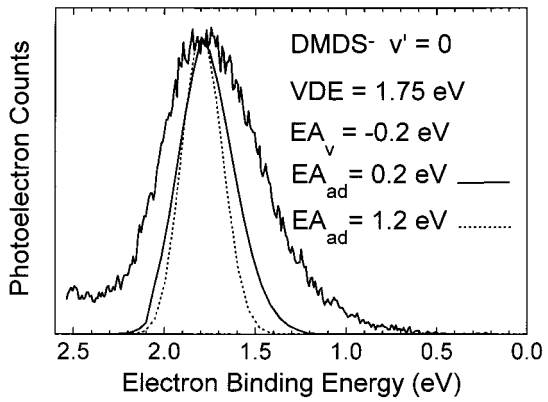

Figure 4. Franck−Condon calculations for the modeling of the dimethyl disulfide photoelectron spectrum. Only the anion vibrational ground state is considered for two very different values of the adiabatic electron affinity EA_{ad}. See text for discussion.

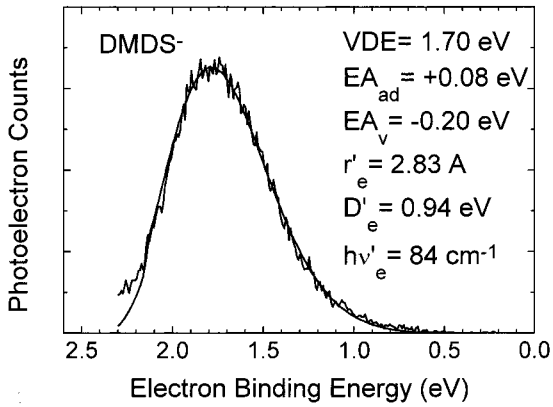

Figure 5. Best fit of the dimethyl disulfide photoelectron spectrum obtained, using energetic and structural parameters as indicated and an estimated anion temperature of 150 K.

we had but one benchmark for EA_{ad} of DMDS. This came from the afterglow experiments of Rinden,[26] in which electron transfer was observed from NO^- anions to DMDS, leading to CH_3S^- fragment[27] and to $DMDS^-$ intact ions. These intact anions undergo fast electron transfer to O_2, and from the known electron affinities of NO and O_2, these results led to a bracketing of the EA_{ad} value for DMDS between +0.02 and +0.45 eV. An examination of the three photoelectron spectra in Figure 2 reveals that extrapolating the low EBE portion of these spectra to zero intensity implies EA_{ad} values between 1.1 and 1.3 eV, in contradiction with the above bracketing. This, together with the fact that these spectra are rather broad, indicating a large geometry change between neutral and anion structures, suggests that the photodetachment process in these cases may not access the ground-state rovibrational level of the neutral disulfides, due to a poor Franck−Condon overlap between the neutral and anion ground states.

Thus, to extract the EA_{ad} values from these spectra, we turned to fitting their Franck−Condon profiles. We performed such calculations on DMDS, taking into account only the S−S stretch, which is the most affected coordinate during the electron attachment process. Potential energy curves are represented by Morse potentials which parameters are fitted to the following experimental or theoretical data (see Tables 1 and 2). For the neutral molecule, we take the dissociation energy (D_e) as 2.7 eV, the equilibrium distance (r_e) as 2.07 Å, and the harmonic vibrational frequency ($h\nu_e$) as 510 cm^{-1}. For the anion potential curve, we set the dissociation energy to EA_{ad} + AE, where AE = 0.86 eV is the measured appearance energy of CH_3S^- from DEA experiments on DMDS.[17] This value is further confirmed by the difference between the S−S bond dissociation energy (2.7−2.8 eV, see Table 2) and the well-known electron affinity of the radical CH_3S (1.86 eV[28]). In a first stage, EA_v has been set to −0.2 eV, even if this value is probably an upper bound (see above), and the VDE to the present measured value of 1.75 eV. The results of this first set of potential parameters are shown in Figure 4 for two very different EA_{ad} values of +1.2 eV and +0.2 eV. In these calculations, we considered only totally relaxed DMDS anions, i.e., only the lowest initial $v' = 0$ vibrational anion state is taken into account. With this first approximation, it is seen that, even for a low EA_{ad} value of +0.2 eV, the Franck−Condon factors begin to be nonzero only for EBE larger than 1 eV. This is due to the important stretching of the equilibrium S−S distance upon electron attachment, making the overlap between the vibrational ground states of the neutral and of the anion extremely small.

The contribution of vibrational hot bands, i.e., initial occupied vibrational anion states v' different from zero present in the beam, must thus be included in the Franck−Condon analysis. We also studied the influence of the three energetic anion parameters. For VDE, the best fitting value remains 1.70 eV, i.e., very close to the experimentally observed peak (1.75 eV). For EA_v, it is not possible to obtain good fits for large negative values, i.e., $EA_v = -1.04$ eV[17] or $EA_v = -1.5$ eV (present calculations). Fits become good only when EA_v is less negative than about −0.5 eV, in agreement with our above estimate. Similarly, good fits are obtained only when EA_{ad} is positive but small. The best fit we obtained indeed corresponds to VDE = 1.7 eV, $EA_v = +0.03$ eV and $EA_{ad} = +0.30$ eV, with a temperature in the anion source of ≈150 K. Because, from the RETS data, it is very unlikely that EA_v could be positive, we set EA_v to −0.2 eV and we obtain a fit of similar quality for VDE = 1.70 eV and $EA_{ad} = +0.08$ eV, as displayed in Figure 5. These values correspond to the following anion potential parameters: equilibrium S−S distance, r_e, of 2.83 Å, dissociation energy, D_e, of 0.94 eV, and anion S−S stretch frequency, $h\nu_e'$, of 84 cm^{-1}. At the estimated temperature of 150 K, several anion vibrational states can be then populated, leading to a broadening of the model spectrum and to a good fit of the experimental data.

The results of this last fit compare well with the present ab initio results (see Tables 1 and 2). For the adiabatic electron affinity EA_{ad} of DMDS, we obtain −0.08, and +0.12 eV, respectively at the MP2/6-31+G* and the MP2/6-311+G(2d, 2p) levels, and +0.35 at the DFT/6-31+G* level. The use of a very large basis set clearly improves the stability of the negative ion, and the second MP2 value is probably very close to the actual value, while the DFT result is probably overestimated. Calculated VDE values are also in good agreement with experimental data and also improve with the size of the basis set. At the highest level of theory (MP2/6-311+G(2d, 2p)), the calculated dissociation energy D_e of the S−S bond is equal to 2.68 eV for neutral DMDS, whereas the experimental value is 2.82 eV.[28] That of the anion is 1.16 eV, i.e., less than half the neutral value, which is rather typical of the σ three-electron bonds.[19] As expected, the major structural change is for the S−S bond length r_e (Table 2): in neutral DMDS, the calculated value is 2.07 Å, as compared to the experimental data of 2.038 Å,[29] while it is 2.74 Å for the anion, i.e., more than 30% of lengthening. As indicated in Table 3, the S−C bond and the dihedral angle C−S−S−C are almost unaffected upon electron attachment, whereas the bond angle S−S−C is slightly decreased. For DEDS, MP2 calculations lead to energetic and

TABLE 3: Other Structural Data for Dimethyl Disulfide (DMDS)

disulfide species	S−C length (Å) MP2[a]/MP2[b]	S−S−C bond angle (°) MP2[a]/MP2[b]	C−S−S−C dihedral angle (°) MP2[a]/MP2[b]
DMDS neutral	1.814/1.818	102.1/101.4	84.0/84.5
	1.81[c]	102.8[c]	84.7[c]
DMDS anion	1.819/1.824	88.8/88.4	86.6/85.6

[a] 6-31+G* basis set. [b] 6-311+G(2d, 2p) basis set. [c] Experimental value from microwave spectroscopy.[29]

structural parameters very similar to those for DMDS and no important change is thus expected for DPDS. DFT results for EA_{ad} seem to be even more overestimated, suggesting that this method is not suitable in the present case of three-electron bonds.

On the other hand, ab initio results for the vertical electron affinities EA_v seem to be too negative to be compatible with the RETS observations and the fitting of the PES spectra. In addition, the harmonic S−S bond stretch anion frequency resulting from our best fit (84 cm^{-1}) is more than twice lower than the calculated MP2 value (216 cm^{-1}). In the Franck−Condon calculations, more negative EA_v values lead to higher S−S anion frequencies but to poor fits (as in Figure 4) of the PES spectra because the contribution of vibrational hot bands is then too small, as outlined above. It is thus likely that other low-frequency vibrational modes, such as that of the S−S−C bond angle, should have to be included to obtain a better Franck−Condon analysis. Also, the anion potential curve, taken here as a Morse potential, may have to be refined so that it allows for a steeper repulsion if the Franck−Condon region while maintaining a similar shape of the anion potential curve at larger distances.

4. Conclusion

Low-energy electron attachment to disulfide bonds has been investigated on a series of model molecules. From RETS experiments, it appears that these compounds form stable anions but do not capture thermal nearly zero energy electrons when they are isolated; they do so only when they are imbedded in clusters. From NIPES experiments, the anion stability is further confirmed and vertical detachment energies have been measured together with the Franck−Condon profile. By fitting this profile, it has been shown that the measured photoelectron spectra are compatible with positive but low adiabatic electron affinity EA_{ad} values, about +0.1 eV, as calculated by ab initio calculations.

Acknowledgment. The authors thank P. D. Burrow, B. Braida, and P. C. Hiberty for very fruitful discussions. K.H.B. acknowledges support from the U.S. National Science Foundation under grant number CHE-9816229. C.H.-L. and J.B. acknowledge IDRIS for providing computer facilities and technical assistance (project no. 990268).

References and Notes

(1) Dai, S.; Schwendmayer, C.; Schürmann, P.; Ramaswamy, S.; Eklund, H. *Science* **2000**, *287*, 655.

(2) Chen, J.; Song, J. L.; Chang, S.; Wang, Y.; Cui, D. F.; Wang, C. C. *J. Biol. Chem.* **1999**, *274*, 19601.

(3) Sun, X.; Dai, Y.; Liu, H.; Chen, S.; Wang, C. *Biochim. Biophys. Acta* **2000**, *45*, 1481.

(4) Barbitz, S.; Jacob, U.; Glocker, M. O. *J. Biol. Chem.* **2000**, *275*, 18759.

(5) Nakamura, H.; Nakamura, K.; Yodoi, J. *Annu. Rev. Immunol.* **1997**, *15*, 351.

(6) Powis, G.; Gaskada, J. R.; Berggren, M.; Kirkpatrick, D. L.; Engman, L.; Cotegreave, I. A.; Angulo, M.; Baker, A. *Oncol. Res.* **1997**, *6*, 303.

(7) Baker, A.; Payne, C. M.; Briehl, M. M.; Powis, G. *Cancer Res.* **1997**, *57*, 5162.

(8) Gallegos, A.; Berggren, M.; Gaskada, J. R.; Powis, G. *Cancer Res.* **1997**, *57*, 4965.

(9) Lmoumène, E. H.; Comte, D.; Jacquot, J. P.; Houée-Levin, C. *Biochemistry* **2000**, *39*, 9295.

(10) Favaudon, V.; Tourbez, H.; Houée-Levin, C.; Lhoste, J. M. *Biochemistry* **1990**, *29*, 10978.

(11) Bergès, J.; Kassab, E.; Comte, D.; Adjadj, E.; Houée-Levin, C. *J. Phys. Chem. A.* **1997**, *101*, 7809.

(12) Loo, J. A.; He, J. X.; Cody, W. L. *J. Am. Chem. Soc.* **1998**, *120*, 4542.

(13) Valentine, S. J.; Anderson, J. G.; Ellington, A. D.; Clemmer, D. E. *J. Phys. Chem. B* **1997**, *101*, 3891.

(14) Velasquez, I.; Reimann, C. T.; Tapia, O. *J. Phys. Chem.* **2000**, *104*, 2546.

(15) Zubarev, R. A.; Horn, D. M.; Fridrikson, E. K.; Lehhler, N. L.; Kruger, N. A.; Lewis, M. A.; Carpenter, B. K.; McLafferty, F. W. *Anal. Chem.* **2000**, *72*, 563.

(16) Zubarev, R. A.; Kruger, N. A.; Fridriksson, E. K.; Lewis, M. A.; Horn, D. M.; Carpenter, B. K.; McLafferty, F. W. *J. Am. Chem. Soc.* **1999**, *121*, 2857.

(17) Modelli, A.; Jones, D.; Distefano, G.; Tronc, M. *Chem. Phys. Lett.* **1991**, *181*, 361.

(18) Morihashi, K.; Kushihara, S.; Inadomi, Y.; Kikuchi, O. *Theochem.* **1997**, *418*, 171.

(19) Braida, B.; Hiberty, P. C. *J. Phys. Chem. A* **2000**, *104*, 4618.

(20) Desfrançois, C.; Abdoul-Carime, H.; Khelifa, N.; Schermann, J. P.; Brenner, V.; Millié, P. *J. Chem. Phys.* **1995**, *102*, 4952.

(21) Hendricks, J. H.; Lyapustina, S. A.; Clercq, H. L. d.; Bowen, K. H. *J. Chem. Phys.* **1998**, *108*, 8.

(22) Frisch, M. J.; Trucks, G. W.; Schlegel, H. B.; Gill, P. M. W.; Johnson, B. G.; Robb, M. A.; Cheeseman, J. R.; Keith, T.; Petersson, G. A.; Montgomery, J. A.; Raghavachari, K.; Al-Laham, M. A.; Zakrzewski, V. G.; Ortiz, J. V.; Foresman, J. B.; Cioslowski, J.; Stefanov, B. B.; Nanayakkara, A.; Challacombe, M.; Peng, C. Y.; Ayala, P. Y.; Chen, W.; Wong, M. W.; Andres, J. L.; Replogle, E. S.; Gomperts, R.; Martin, R. L.; Fox, D. J.; Binkley, J. S.; Defrees, D. J.; Baker, J.; Stewart, J. P.; Head-Gordon, M.; Gonzalez, C.; Pople, J. A. *Gaussian 94*, Gaussian, Inc.: Pittsburgh, PA, 1995.

(23) Bergès, J.; Furster, F.; Jacquot, J. P.; Silvi, B.; Houée-Levin, C. *Nukleonika* **2000**, *45*, 23.

(24) Harth, K.; Rüf, M.-W.; Hotop, H. *Z. Phys.* **1989**, *D14*, 149.

(25) Desfrançois, C.; Khelifa, N.; Lisfi, A.; Schermann, J. P. *J. Chem. Phys* **1992**, *96*, 5009.

(26) Rinden, E.; Maricq, M. M.; Grabowski, J. J. *J. Am. Chem. Soc.* **1989**, *111*, 1203.

(27) Stirk, K. M.; Orlowski, J. C.; Leeck, D. T.; Kenttäma, H. I. *J. Am. Chem. Soc.* **1992**, *114*, 8604.

(28) Lide, D. R. *CRC Handbook of Chemistry and Physics*; CRC Press: Boca Raton, 1995; Vol. 74.

(29) Landolt-Börnstein *Numerical Data and Functional Relationships in Science and Thechnology*; Springer-Verlag: Berlin, 1987; Vol. 7.

(30) Derreumaux, P.; Vergoten, G. *J. Chem. Phys.* **1995**, *102*, 8586.